Shape Optimization of Wideband Antennas for Microwave Energy Harvesters Using FDTD

Takuya Mori[1], Ryo Murakami[1], Yuki Sato[1], Felipe Campelo[2] and Hajime Igarashi[1]

[1]Graduate School of Information Science and Technology, Hokkaido University, 060-0814, Sapporo, Japan
[2]Universidade Federal de Minas Gerais, Departamento de Engenharia Eletrica, Belo Horizonte 31270-901, Brazil.

This paper presents parameter and topology optimizations of wideband antennas for microwave energy harvesters based on FDTD computations. The antenna shapes are optimized to reduce return losses in a specific frequency band using micro genetic algorithm. The shape parameters of a two-arm planar spiral antenna (PSA) are optimized. Moreover, topology optimization is performed using normalized Gaussian network, where spatial symmetries are assumed. It is shown that the return losses of the optimized antennas are less than -10dB from 1.0GHz to 2.0GHz in which they have isotropic directivity.

***Index Terms*—Topology optimization, normalized Gaussian network (NGnet), Group Theory, FDTD method, energy harvesting.**

I. Introduction

In recent years wireless sensors have attained great attentions for monitoring health and safety condition of constructions and natural environments. When wireless sensors have batteries as their power supply, it is laborious and expensive to charge batteries of wireless sensors located in difficult access environments. Energy harvesting allows us to realize wireless sensors which can operate autonomously.

Energy harvesters absorb energy from ambient environment. Many kinds of energy harvesters have been developed so far [1-3] because there are diverse forms of environmental energy such as sunlight, temperature difference and vibration.

The key element of a microwave energy-harvesting system is the rectenna [4] which consists of a receiving antenna and rectifier which converts the microwaves into DC power. For the efficient power absorption, various antenna shapes have been proposed [2] [5-6]. For uniform directivity, point, left-right and rotational symmetries have been introduced to the antenna [7-9]. There are, however, few works where the shape of antennas for energy harvesters is optimized by metaheuristic approaches to realize wideband operations.

In this paper, we present the parameter and topology optimizations based on micro genetic algorithm (μGA) [10] to realize wideband antennas for energy harvesters. The return loss in a specified frequency band is minimized. The antenna properties are analyzed using FDTD method. The design parameters of a two-arm spiral antenna are optimized. Moreover, we perform topology optimization of the antenna using normalized Gaussian network (NGnet) [11] in which the antenna shape is expressed in terms of the linear combination of normalized Gaussian functions. We do not need design parameters to represent the shapes for the topology optimization. In our optimization, spatial symmetries are assumed for isotropic directivity. We will report the optimization results and compare the simulated properties with measured results of the manufactured antennas.

Manuscript received May 23, 2014. Corresponding author: T. Mori (e-mail: tmori@em-si.eng.hokudai.ac.jp).
Digital Object Identifier inserted by IEEE

II. Antenna analysis

In this work, the frequency characteristics of antennas are computed using FDTD method [12] by which the frequency response in a wide frequency band can easily be computed. Let us consider the Maxwell equations

$$\nabla \times \boldsymbol{E} + \mu \frac{\partial \boldsymbol{H}}{\partial \boldsymbol{t}} = 0 \tag{1a}$$

$$\nabla \times \boldsymbol{H} - \varepsilon \frac{\partial \boldsymbol{E}}{\partial \boldsymbol{t}} = \boldsymbol{J} \tag{1b}$$

where $\boldsymbol{E}$, $\boldsymbol{H}$, $\boldsymbol{J}$, μ and ε are electric field, magnetic field, current density, permeability and permittivity, respectively. Equation (1) is discretized with FDTD method in which time and space derivatives are approximated by central finite differences to obtain

$$\boldsymbol{E}^{n} = \frac{1-\dfrac{\sigma\Delta t}{2\varepsilon}}{1+\dfrac{\sigma\Delta t}{2\varepsilon}}\boldsymbol{E}^{n-1} + \frac{\dfrac{\Delta t}{\varepsilon}}{1+\dfrac{\sigma\Delta t}{2\varepsilon}}\nabla\times\boldsymbol{H}^{n-\frac{1}{2}} \tag{2a}$$

$$\boldsymbol{H}^{n+\frac{1}{2}} = \boldsymbol{H}^{n-\frac{1}{2}} + \frac{\mu}{\Delta t}\nabla\times\boldsymbol{E}^{n} \tag{2b}$$

where n and σ denote time step and conductivity. In the FDTD method, (2a) and (2b) are calculated alternately. The input impedance of the antennas are computed from the Fourier transform of the input voltage and current as follows:

$$Z_{\text{in}}(f) = \frac{F[V_{\text{in}}(t)]}{F[I_{\text{in}}(t)]} \tag{3}$$

where $V_{\text{in}}(t)$ and $I_{\text{in}}(t)$ are the feeding voltage and current obtained by the FDTD analysis.

III. Optimization Method

A. Parameter optimization

We consider the two-arm PSA using μGA because it has broad bandwidth characteristics [6]. In this study, design parameters are defined as shown in Fig. 1 and the optimization

is conducted by changing them using μGA. The two-arm PSA has 2-fold rotational symmetry, namely, that is identical after 360/2 degree rotation. This symmetry is expressed by the point group C_2 [13], that is,

$$C_2 = (e, a) \tag{4}$$

where e and a represent the identity operation and counter clockwise rotation of 360/2 degrees around a feeding point, respectively.

B. *Topology optimization*

1) *Representation of antenna shape*

In the topology optimization, we can flexibly change the antenna shapes. However, the antenna for energy harvesting, in which we cannot assume any polarization in microwaves, should have spatial symmetry to have isotropic directivity. For this reason, we assume C_2 and the following symmetries:

$$D_1 = (e, b) \tag{5a}$$

$$C_4 = (e, a, a^2, a^3) \tag{5b}$$

$$D_2 = (e, a, b, ba) \tag{5c}$$

In the groups C_n and D_n, a and b denote 360/n degree rotation around the center in the two-dimensional plane, and fold around the central horizontal axis. Fig. 2 depicts the shapes which have the above symmetries. The shape in the unit region, symbolized by "*F*", is optimized. There is redundancy in the symmetric assumptions because C_4- and D_2-symmetric shapes also have C_2 and D_1 symmetries, respectively.

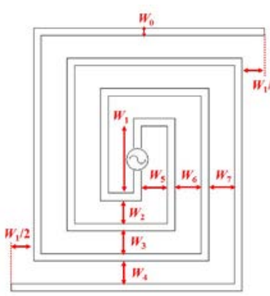

Fig. 1 Design parameters of PSA

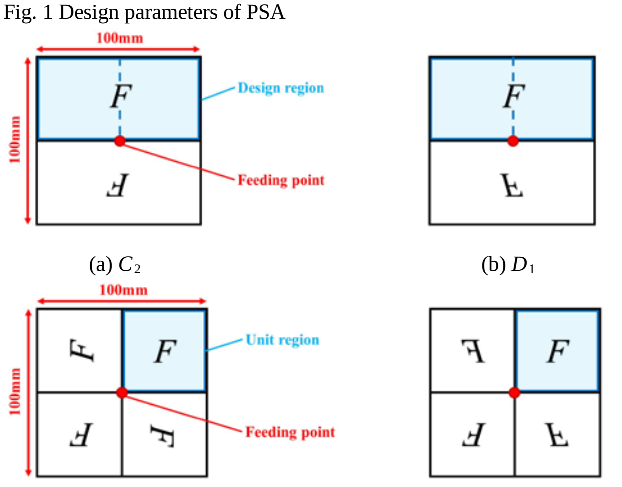

(a) C_2 (b) D_1

(c) C_4 (d) D_2

Fig. 2 Symmetry of antennas

It is difficult to find the global optimum in the topology optimization which has high DoFs. Even if the global optimum has, for example, C_4 symmetry, it would be difficult to find it assuming C_2 symmetry. This is the reason why we consider C_4 and D_2 symmetries.

2) *Optimization method*

For the topology optimization, we employ the NGnet whose output is given by the linear combination of the normalized Gaussian functions shown in Fig. 3, that is,

$$y(\boldsymbol{x}) = \sum_{i=1}^{N} w_i b_i(\boldsymbol{x}) \tag{6a}$$

$$b_i(\boldsymbol{x}) = G_i(\boldsymbol{x}) \Big/ \sum_{k=1}^{N} G_k(\boldsymbol{x}) \tag{6b}$$

where $G_k(\boldsymbol{x})$ and $\boldsymbol{w}_i$ denote the Gaussian function and weighting coefficient, respectively. We uniformly deploy 81 Gaussians in the square unit region as shown in Fig. 4. For models in (a) and (b) in Fig.2, we place two square unit regions. The standard deviation in the Gaussian is set to 50/16 mm. The size of the FDTD cells is set to 1mm. The perfect conductor condition is imposed to the surface of the FDTD cell corresponding to the antenna. The state s_e of each FDTD-cell surface is determined from the output of the NGnet at its center $\boldsymbol{x}_e$ as follows:

$$s_e = \begin{cases} \text{conductor} & y(\boldsymbol{x}_e) \geq 0 \\ \text{air} & y(\boldsymbol{x}_e) < 0 \end{cases} \tag{7}$$

The optimization is conducted by changing the value of w_i in (6a) using μGA.

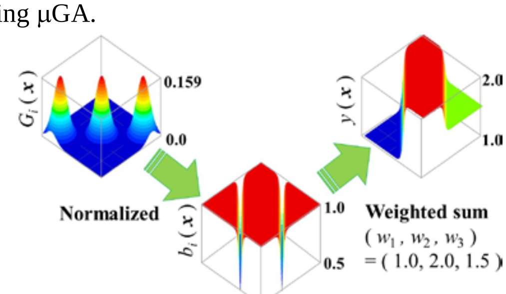

Fig. 3. Gaussians, normalized Gaussians, and output of NGnet.

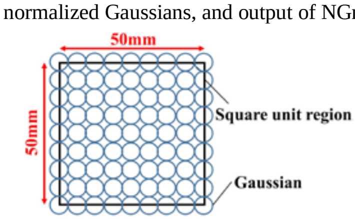

Fig. 4. Gaussians distributed in square unit region

IV. Optimization Problem

The aim of those optimizations is to minimize the return loss of the antenna loaded by a 50Ω transmission line in a specified frequency range. The optimization problem is defined by

$$< S_{11} > = \int_{f_0}^{f_1} S_{11}(f) df \Big/ (f_1 - f_0) \rightarrow \min. \tag{8a}$$

where

$$S_{11}(f) = 20\log_{10}\left|\frac{Z_{\text{in}}(f) - Z_0}{Z_{\text{in}}(f) + Z_0}\right| \tag{8b}$$

and $Z_{\text{in}}(f)$ and $S_{11}(f)$ are the input impedance and return loss of the antenna. The values of Z_0, f_0 and f_1 are set to 50Ω, 1.0GHz, 2.0 GHz, respectively. In the analysis, the antenna is assumed to have infinitely thin metallic surface which is loaded by a dielectric sheet of 2mm thick and $\varepsilon_r = 4$. Moreover, a feeding point is assumed to be at the center of the design region. The computational times for the parameter and topology optimization are almost identical. In μGA, the number of individuals is set to 8 and the optimization is conducted over 100 generations. In this setting it takes about 3 days to obtain final solution using the *Intel Xeon CPU* (2.4GHz, 4 cores).

V. Optimization Results

The results of the optimization are summarized in Table I. For reference, the result of the topology optimization without assumption of symmetry is included (represented by E). It is found that the best fitness is obtained for D_1 symmetry. There are no significant differences in the fitness values for the two-arm PSA and C_4-, C_2-, D_2-symmetric antennas. We find that the D_1- and D_2-symmetric solutions have anisotropic directivities. Moreover, we find that C_2-symmetric antenna has rather narrow band. For this reason, we choose PSA and C_4-symmetric antenna for further considerations. Figure 5 shows the shapes of these two antennas, while the shapes with other symmetry are shown in Fig. 6 for reference. The C_4-symmetric antenna has a floating metal which surrounds the four-arm metal connected to the feeding point. We manufacture these antennas on the dielectric substrate (NZ-G31KR) which are shown in Fig.7.

The return losses S_{11} are plotted as a function of frequency in Fig. 8. The measurement results for the manufactured antennas are also plotted, where they are measured by E5061B Network Analyzer. We find that both return losses are lower than -10dB from 1GHz to 2GHz. There are some discrepancies between the computed and measured profiles. These discrepancies would be attributed to deviation in the permittivity in the substrate and metallic loss. We also find two clear resonances in the profile of the two-arm PSA, whereas C_4-symmetric antenna has rather flat profile.

The radiation patterns obtained by FDTD analysis are shown in Figs. 9 and 10. Both are found to have almost isotropic directivities which are suitable for energy harvesting.

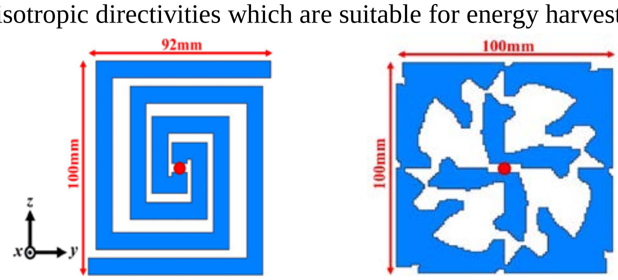

(a) two-arm PSA (parameter optimization)   (b) C_4-symmetric antenna (topology optimization)

Fig. 5 Selected optimized antennas

Table I
Results of Optimization

Symmetries	$<S_{11}>$	Directivity $(E_{\max}/E_{\min})^2$ (xy-plane, xz-plane) [dB]
E	-7.68	(-10.5, -8.6)
C_2	-13.72	(-12.6, -6.7)
D_1	-19.00	(-13.7, -34.2)
D_2	-14.39	(-2.6, -38.2)
two-arm PSA*	-14.49	(-5.0, -13.9)
C_4	-14.81	(-5.7, -14.8)

* $(W_0, W_1, \ldots, W_7)$ = (8.0, 8.0, 4.0, 6.0, 4.0, 2.0, 3.0, 9.0) [mm]

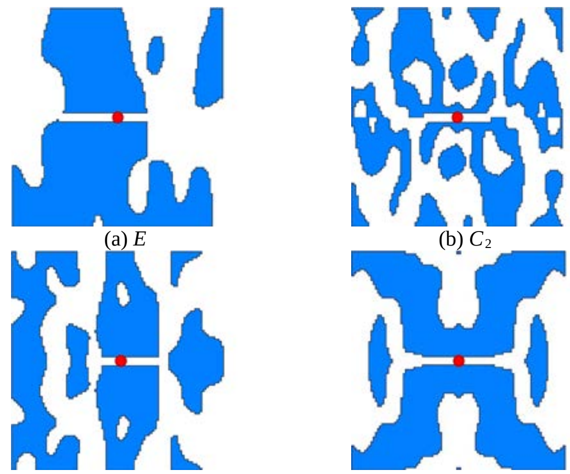

(a) E (b) C_2 (c) D_1 (d) D_2

Fig. 6 Antenna Shapes obtained by topology optimization

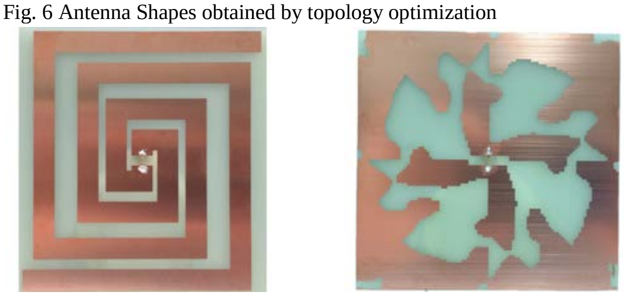

(a) two-arm PSA   (b) C_4-Symmetric antenna

Fig. 7 Manufactured antennas

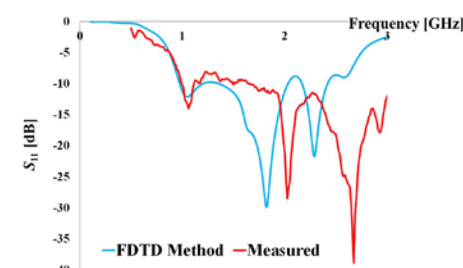

(a) two-arm PSA

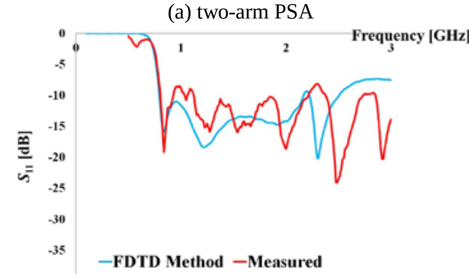

(b) C_4-symmetric antenna

Fig. 8 Return losses S_{11}

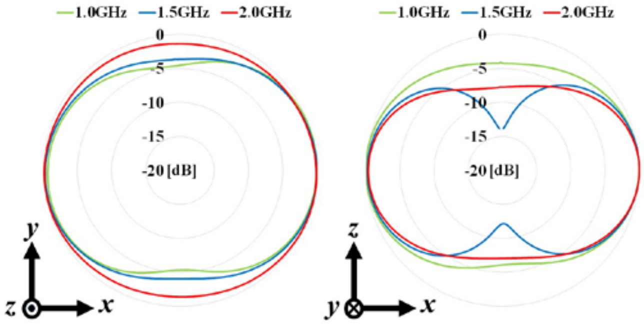

(a) *xy*-plane (b) *xz*-plane

Fig. 9 Radiation pattern of two-arm PSA (computed)

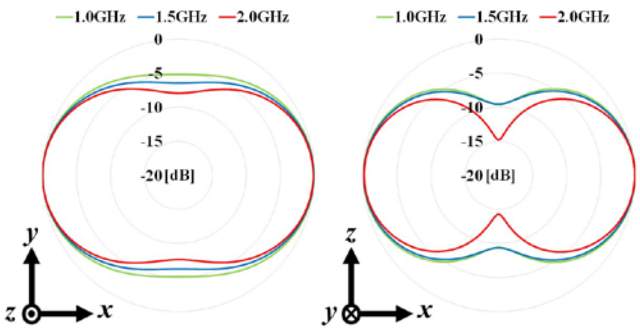

(a) *xy*-plane (b) *xz*-plane

Fig. 10 Radiation pattern of C_4-symmetric antenna (computed)

Current density distributions are shown in Figs. 11 and 12 at 1.0 GHz and 2.25GHz. We can see in these figures that there are local currents concentrating near the feeding point at 1GHz while the global currents exist at 2.25GHz. For wide frequency operations, we need sufficiently rich complexity in the antenna shape, which are realized by the topology optimization.

VI. Conclusion

In this paper, we have proposed two kinds of antennas for energy harvesters obtained by parameter and topology optimization. The shape parameters of the two-arm PSA are optimized. Moreover, topology optimization is performed assuming spatial symmetries to have isotropic directivity. The measured and computed return losses are lower than -10dB from 1GHz to 2GHz. The optimized two-arm PSA and C_4 symmetric antenna have almost the same performance. We plan to develop antennas which have more wide operating range using the present topology optimization.

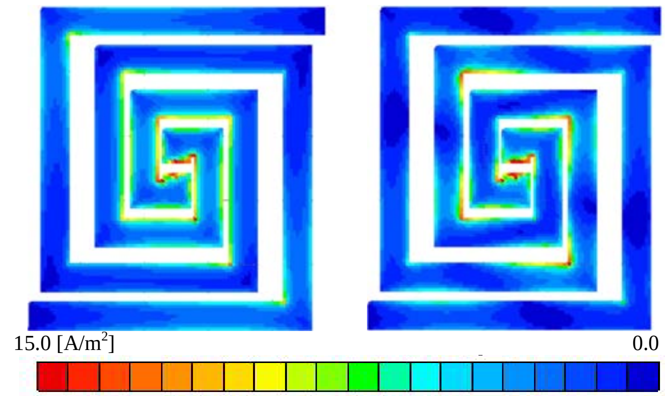

(a) 1.0GHz (b) 2.25GHz

Fig. 11. Current distribution of two-arm PSA.

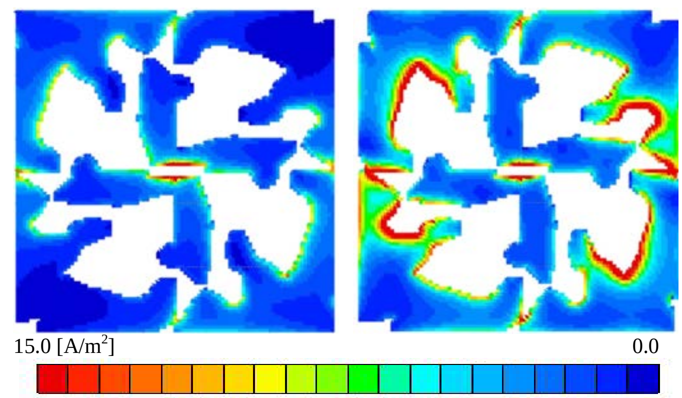

(a) 1.0GHz (b) 2.25GHz

Fig. 12. Current distribution of C_4-symmetric antenna.

References

[1] L. C. Blystad, E. Halvorsen, and S. Husa, “Piezoelectric MEMS energy harvesting systems driven by harmonic and random vibrations,” *IEEE transactions on ultrasonics, ferroelectrics, and frequency control*, vol. 57, Apr. 2010, pp. 908-19

[2] D. Bouchouicha, F. Dupont, M. Latrach, L.Ventura, “Ambient RF Energy Harvesting," *International Conference on Renewable Energies and Power Quality (ICREPQ’10)*, March, 2010

[3] C. Lu, V. Raghunathan, and K. Roy, “Maximum Power Point Considerations in Micro-Scale Solar Energy Harvesting Systems,” *ISCAS 2010*, pp. 273-276

[4] H. Sun, Y. Guo, He, and Z. Zhong, “Design of a High-Efficiency 2.45-GHz rectenna for Low-Input-Power Energy Harvesting,” *IEEE Antennas amd Wireless Propagation Letters*, vol. 11, pp. 929-932, 2012

[5] M. K. Hosain, A. Z. Kouzani, Susannah J. Tye, O. A. Abulseoud, and M. Berk, “Design and Analysis of an Antenna for Wireless Energy Harvesting in a Head-mountable DBS Device,” *35th Annual International Conference of the IEEE EMBS Osaka*, Japan, 3-7 July, 2013

[6] Z. Zakaria, N. A. Zainuddin, M. Z. A. Abd Aziz, M N. Husain, M. A. Mutalib, “Dual-Band Monopole Antenna For Energy Harvesting System,” *2013 IEEE Symposium on Wireless Technology and Applications (ISWTA)*, September 22-25, 2013, Kuching, Malaysia

[7] H. Nakamo, H. Yasui, and J. Yamauchi, “Numerical analysis of two-arm spiral antennas printed on a Finite-size dielectric substrate," *IEEE Trans. Antennas Propag.*, Vol. 50, No. 3, pp.362-370, 2002.

[8] X. Quan, R. L. Li and M. M. Tentzeris, “a novel broadband omni-directional circularly polarized antenna for mobile communications”, *in IEEE International Symposium on Antennas and Propagation*, 2011, pp.1777-1779

[9] G. Kang, Z. Du, and K. Gong, “Compact broadband printed Slot-Monopole-Hybrid diversity antenna for mobile terminals”, *IET Microw. Antennas Propag.*, vol. 3, no.1, pp. 47-54, 2009.

[10] C. Coello and G. Pulido, “A Micro-Genetic Algorithm for Multiobjective Optimization,” Lecture Notes in Computer Science, Volume 1993, pp. 126-140, 2001

[11] J. Moody, “Fast Learning in Networks of Locally-Tuned Processing Units,” *Neural Computation*, vol. 1, No. 2, pp. 281-294, 1989.

[12] A. Taflove. *Computational Electrodynamics: The Finite Difference Time-Domain Method*. Norwood, MA: Artech House, 1996

[13] R. McWeeny, *Symmetry*: *An Introduction to Group Theory and Its Applications*, Courier Dover Publications, 2002.